Biogeosciences Discuss., 10, 2245–2267, 2013
www.biogeosciences-discuss.net/10/2245/2013/
doi:10.5194/bgd-10-2245-2013

Biogeosciences
Discussions
Open Access

A new estimate of ocean oxygen utilization points to a reduced rate of respiration in the ocean interior

O. Duteil[1], W. Koeve[1], A. Oschlies[1], D. Bianchi[2], I. Kriest[1], E. Galbraith[2], and R. Matear[3]

[1]GEOMAR, Helmhotz Center for Ocean Research Kiel, Düsternbrooker Weg 20, 24103 Kiel, Germany
[2]Department of Earth and Planetary Science, McGill University, Montreal, QC, Canada
[3]CSIRO Marine and Atmosphere Research, Hobart, TAS, Australia

Received: 17 January 2013 – Accepted: 21 January 2013 – Published: 8 February 2013

Correspondence to: O. Duteil (oduteil@geomar.de) and W. Koeve (wkoeve@geomar.de)

Published by Copernicus Publications on behalf of the European Geosciences Union.

Abstract

The Apparent Oxygen Utilization (AOU) is a classical measure of the amount of oxygen respired by biological processes in the ocean interior. We show that the AOU systematically overestimates the True Oxygen Utilization (TOU) in 6 coupled circulation-biogeochemical ocean models, due to atmosphere–ocean oxygen disequilibrium in the subduction regions, consistent with prior work. We develop a new approach that we call Evaluated Oxygen Utilization (EOU), which approximates the TOU at least twice as well as AOU in all 6 models, despite large differences in the physical and biological components of the models. Applying the EOU approach to a global observational dataset leads to an estimated biological oxygen consumption rate that is by 25 percent lower than that derived from AOU-based estimates.

1 Introduction

Respiration is a key biological process in the ocean. Classically, respiration in the interior of the ocean is quantified by the "Apparent Oxygen Utilization" (AOU) (e.g. Redfield et al., 1963; Anderson and Sarmiento, 1995; Pahlow and Riebesell, 2000; Feely et al., 2004; Sarmiento and Gruber, 2006; Keeling et al., 2010; Duteil et al., 2012). The AOU concept assumes that sea-surface oxygen is fully equilibrated with the atmosphere with concentrations close to saturation level. This is, however, only approximately true, as physical and chemical processes occurring in regions of water mass formation can lead to significant undersaturation in surface waters that are subducted into the ocean interior (e.g. Gordon and Huber, 1990; Koeve, 2001; Russell and Dickson, 2003; Koertzinger et al., 2005; Keeling et al., 2010).

Here, we develop a new diagnostic, which we refer to as "Evaluated Oxygen Utilization" (EOU), and which is based on the assumption of an isopycnal propagation of the surface ocean oxygen undersaturation into the interior of the ocean. Our approach is tested in 6 coupled biogeochemical-physical models, where the oxygen respired since the water's last contact with the atmosphere (True Oxygen Utilization, TOU) is computed explicitly using an idealized passive tracer of preformed oxygen (Ito et al., 2004). Finally, AOU and EOU diagnostics are computed from a global observational dataset, allowing the concentrations of regenerated and preformed nutrients to be determined (Ito and Follows, 2005)

2 Methods

2.1 Oxygen utilization

The Oxygen Utilization (OU) is generally defined as the difference between the so called "preformed" oxygen and the actual oxygen concentration observed at a given point in the interior of the ocean, i.e. $OU = O_{2\ pre} - O_{2\ obs}$. Preformed oxygen is the oxygen concentration that a water parcel had at the time of its last contact with the atmosphere, just before it was subducted into the ocean interior. Preformed oxygen, however, is not known a priori and cannot be directly measured away from the ocean surface. In this study the preformed oxygen concentration has been estimated in three different ways, leading to three different formulations of oxygen utilization:

- Apparent Oxygen Utilization (AOU). The traditional concept of AOU assumes that preformed oxygen corresponds to the oxygen saturation concentration, $O_{2\ sat}$, given by the in situ potential temperature and salinity. An implicit assumption in this approach is that waters are fully saturated in regions where subduction occurs. Although this has always been recognized as an incorrect approximation (hence the term apparent), the approach has been widely used (e.g. Redfield et al., 1963; Anderson and Sarmiento, 1995; Pahlow and Riebesell, 2000; Feely et al., 2004; Sarmiento and Gruber, 2006; Keeling et al., 2010; Duteil et al., 2012).

- True Oxygen Utilization (TOU). In numerical models, the preformed oxygen concentration can be calculated explicitly using an idealized preformed oxygen tracer.

BGD
10, 2245–2267, 2013

At the sea surface, during every model time step, this tracer is restored to the model's oxygen concentration. In the interior of the ocean the preformed oxygen tracer is passively transported by advection and diffusion, with no biological sinks or sources affecting its concentration. Substracting the actual oxygen concentration from the preformed oxygen tracer yields the TOU. This approach is identical to that of Ito et al. (2004).

– Evaluated Oxygen Utilization (EOU). In this new diagnostic, we correct for deviations from complete oxygen saturation in subduction regions in a pragmatic way that can be straightforwardly applied to any model output or compilations of oxygen measurements. Considering that transport in the ocean takes place mostly along isopycnal surfaces, we estimate preformed oxygen for each isopycnal layer from the area weighted annual-mean oxygen disequilibrium below the seasonal mixed layer at 100 m water depth (see Appendix for a more detailed description of the method).

As a general remark, mixing of waters with different TS properties usually leads to an increase of the degree of oxygen saturation. The result of this non linearity will then be an underestimation of oxygen utilization in both the AOU or EOU diagnostic. This bias is however small and does not exceed a few percent in the ocean interior (Dietze and Oschlies, 2005).

2.2 Models and datasets

Six global biogeochemical-circulation models are used here (see Table 1 for details): MOM P2A (Gnanadesikan et al., 2004), CSIRO (Matear and Hirst, 2003), om1p7-BLINGv0 (Galbraith et al., 2010), UVIC2.8 (Oschlies et al., 2008), TMM-MIT2.8 (Kriest et al., 2010) and TMM-ECCO2. The first four configurations have been used in previous studies. The TMM-ECCO2 version applies the biogeochemistry of TMM-MIT2.8 but differs by its forcing circulation field. The transport matrix (Khatiwala, 2007) used in the TMM-ECCO2 run has been extracted from the MIT-ECCO2 data assimilation

BGD
10, 2245–2267, 2013

Title Page
Abstract Introduction
Conclusions References
Tables Figures
◂◂ ▸▸
◂ ▸
Back Close
Full Screen / Esc
Printer-friendly Version
Interactive Discussion

experiment (Stammer et al., 2004). All models are forced by prescribed atmospheric conditions in an attempt to obtain realistic pre-industrial circulation fields.

The pelagic ecosystem part of the biogeochemical models ranges from relatively simple nutrient-restoring type (CSIRO, MOM P2A) to intermediate complexity nutrient-phytoplankton-zooplankton-detritus (NPZD) models (om1p7-BLINGv0, UVIC2.8, MIT2.8, ECCO2). All models include an explicit preformed oxygen tracer allowing the computation of the True Oxygen Utilization. Integration time is at least 2000 yr to reach a steady state quasi-equilibrium. Annual mean outputs from these models are compared against objectively analyzed annual means of the World Ocean Atlas (WOA) 2009 (Garcia et al., 2010). Prior to analysis, all model output fields were regridded onto the 33 levels 1 × 1 degree WOA grid.

3 Comparisons of AOU, EOU and TOU

3.1 AOU patterns in observations and models

Patterns of the AOU are often used to characterize the main water masses. In the observations (Fig. 1a), the northern deep Atlantic Ocean AOU displays low values (below 100 $\mathrm{mmol\,m^{-3}}$), because this region is filled with recently formed, young, North Atlantic Deep Water (NADW). As the NADW spreads southward, it mixes with the older Circumpolar Deep Water (CDW) originating from the Southern Ocean, leading to an AOU increase (120 to 160 $\mathrm{mmol\,m^{-3}}$). The deep Pacific Ocean is solely filled by the CDW and AOU tends to increase northwards as waters become older and lose oxygen via remineralization of organic matter. In both oceans, intermediate-depth AOU displays high values (exceeding 200 $\mathrm{mmol\,m^{-3}}$) in the tropical regions, due to the sluggish circulation and the remineralization of large amounts of organic material exported from productive surface waters.

All six models studied here simulate similar global patterns of AOU (Fig. 1b): low values in the NADW (below 100 $\mathrm{mmol\,m^{-3}}$), intermediate AOU in the CDW (between

BGD
10, 2245–2267, 2013

100 to 150 mmol m^{-3}), high values in tropical regions, and a northward increase of AOU in the Pacific Ocean to values higher than 200 mmol m^{-3}. This suggests that the models used in this study do, to first order, realistically represent the combined effects of circulation and biology and are therefore suitable for investigating the large-scale patterns of oxygen utilization in the ocean.

3.2 Evaluation of the AOU approach in models

Comparing AOU and TOU in these models, however, reveals that AOU substantially and systematically overestimates TOU (Fig. 2a). This is because surface waters are not fully saturated upon subduction into the ocean interior, which can arise from several potential mechanisms: mixing with deep, oxygen-depleted waters, limitation of air sea exchange at high latitude due to sea ice, and competition between ocean-atmosphere gas transfer and subduction rate (Ito et al., 2004). This surface oxygen disequilibrium (see Appendix) modifies the amount of "preformed" oxygen, $O_{2\ pre}$, which is transferred into the ocean interior by transport along isopycnals. Because $O_{2\ pre}$ is always less than $O_{2\ sat}$, TOU is always less than AOU. Maximum AOU–TOU differences range from 23 (MIT2.8) to 117 mmol m^{-3} (om1p7-BLINGv0) (CSIRO: 31 mmol m^{-3}, MOM P2A: 61 mmol m^{-3}, ECCO2: 70 mmol m^{-3}, UVIC: 76 mmol m^{-3}). This range of values encompasses the maximum oxygen disequilibrium of 73 mmol m^{-3} found by Ito et al. (2004).

3.3 Evaluation of the EOU approach in models

The widespread AOU–TOU differences simulated by all our models points to a limited reliability of the AOU as a tool to infer oxygen utilization rates in the real ocean. In order to better estimate oxygen utilization in the ocean, we introduce here the EOU diagnostic. The ability to estimate the oxygen utilization at the global or bassin scale is assessed by computing the volume-weighted RMS error for AOU vs. TOU and EOU

BGD
10, 2245–2267, 2013

vs. TOU

$$\mathrm{RMSErr}_X = \sqrt{\sum_i \sum_j \sum_k \left((X - \mathrm{TOU})^2 \times \frac{V_{i,j,k}}{V_{\mathrm{ocean}}} \right)} \tag{1}$$

where X is either AOU or EOU and i, j, k denote the dimensions of the spatial domain. The sums of the square differences are weighted by the relative volume V of the corresponding grid boxes over the total ocean volume. This approach has been used previously in Kriest et al. (2010); Duteil et al. (2012).

The computed RMS error is less than half when EOU is used instead of AOU (Fig. 3) to estimate TOU. This reduction of RMS error holds for all ocean basins.

Regional differences between EOU and TOU are shown in Fig. 2b. In the case of CSIRO and MIT28, the EOU is a very good proxy of the TOU, with the maximum difference of less than 10 mmol m^{-3}. In MOM P2A, UVIC and ECCO2, EOU represents TOU in the Atlantic and Pacific basins in a relative accurate way, with a maximum difference of less than 20 mmol m^{-3}. This difference is higher in om1p7-BLINGv0, with values up to 50 mmol m^{-3} in the deep Pacific Ocean. However, even with this model there is still a halving of the high bias when using EOU instead of AOU (Fig. 2a) to estimate TOU. In UVIC and om1p7-BLINGv0, EOU underestimates (i.e. negative EOU–TOU values) oxygen utilization by 10 to 20 mmol m^{-3} (UVIC) and 10 to 40 mmol m^{-3} (om1p7-BLINGv0) at intermediate depths in the Atlantic Ocean, between 1000 and 2000 m depth.

The EOU approach we suggest here is an ad hoc approximation of true oxygen utilization in the ocean that is designed to be applicable to model outputs and observations a like. As such, the estimate of preformed oxygen in the EOU approach has to simplify processes actually taking place in the ocean. In particular, we assumed that the water is transported solely along isopycnals in the ocean interior and neglected diapycnal processes. Some other simplifying assumptions can however give rise to the discrepancies between EOU and TOU, presented above.

BGD
10, 2245–2267, 2013

First, in the EOU definition, the mean oxygen saturation of any given isopycnal surface is estimated by computing the area-weighted mean oxygen concentration at the intercept of this layer with the 100 m depth horizon. This is only an approximation as in reality waters in the interior of the ocean are variable mixtures of water masses formed in different source regions and having different specific surface oxygen disequilibrium (see Appendix, Fig. B1). On the same isopycnal, waters in for example the North Atlantic will origin mainly from the northern outcrops of this isopycnal, as will be their preformed oxygen content, while waters in the South Atlantic will mainly origin from the Southern Ocean outcrops. Resolving the complexity of variable water mass fractions contributing to the actual preformed oxygen concentration explicitly is a non-trivial task (Gebbie and Huybers, 2011), hence our ad hoc approximation.

Second, our ad hoc approach ignores aspects of seasonality. Water masses form mostly in winter whereas annual mean model outputs have been used in our analysis. In order to reduce the impact of this simplification, we compute the preformed oxygen used for EOU from the mean oxygen disequilibrium of a given isopycnal at 100 m depth rather than the ocean surface. This is guided by the assumption that the upper permanent thermocline is mostly characterized by winter conditions (Stommel, 1979). This assumption provides also a practical and easy solution to better estimate the oxygen utilization from observations, in which high latitudes are biased seasonally, with fewer observations during the winter season.

4 Application of the EOU to observations

Encouraged by the improvements in the determination of oxygen utilization, we now apply the EOU approach to a climatological observational database, the World Ocean Atlas 2009 (WOA). In the deep ocean, between 2000 and 4000 m depth, EOU displays values lower than AOU by about 30 to 40 $\mathrm{mmol\,m^{-3}}$, corresponding to a reduction of about 25 percent of the mean AOU value. In intermediate layers, between 500 and

BGD
10, 2245–2267, 2013

1500 m depth, difference between AOU and EOU reaches 10 to 20 $\mathrm{mmol\,m^{-3}}$ in the tropical Ocean and 40 $\mathrm{mmol\,m^{-3}}$ in the Southern Ocean (Fig. 4a).

This difference in the estimation of oxygen utilization leads to a reassessment of the regenerated vs. total nutrients pool. Regenerated nutrients are transported by biological export production from the surface ocean to the interior, whereas preformed nutrients are transported from the surface to the interior by subduction and sinking (Ito and Follows, 2005; Marinov et al., 2008). The global mean regenerated over total ratio for phosphate, derived from the WOA observations and using the AOU diagnostic, is 0.40. Using a data-constrained ocean circulation and biogeochemistry model and basing their estimate on nutrient export and sequestration since the last contact of the water parcel with the atmosphere, DeVries et al. (2012) proposed a higher value of 0.50. Here we show, using the EOU approach, that the regenerated over total ratio appears to be significantly lower than either prior estimate with a global mean value of 0.30 (Fig. 4b and Table 2). This ratio is 30 percent weaker than what would be determined using the AOU approach in the Southern Ocean (south of 50° S).

As a note of caution, this result should not be generalized to the carbon cycle: the ocean-atmosphere equilibration time for CO_2 is one order of magnitude larger than for oxygen, and surface disequilibrium will have a different and potentially complex effect on carbon storage.

5 Conclusions

The concentration of oxygen in the ocean interior is the result of a competition between circulation dynamics, biological processes and air sea exchanges. We have confirmed, in a comparison of six global models, that the AOU is a biased estimate of the effective respiration (TOU) due to disequilibrium between the surface ocean and atmosphere. The EOU approach consists of estimating the preformed oxygen concentration of a given isopycnal layer by the near surface disequilibrium in regions where the isopycnal layer outcrops. This approach performs better then the AOU in estimating

BGD
10, 2245–2267, 2013

the TOU. We thus recommend to use the EOU approach in studies where an accurate estimate of respiration is of central importance. For instance, the EOU approach could be used in combination with an estimate of water mass ventilation rate in order to infer rates of oxygen consumption in the ocean interior.

Appendix A

Evaluated Oxygen Utilization

In the Evaluated Oxygen Utilization (EOU) diagnostic the estimate of preformed oxygen is based on the concept of the dominance of isopycnal transport in the intermediate and deep ocean. The following procedure is applied individually to the 6 models and finally to the WOA dataset.

We discretisize the ocean into a number of density layers. Pragmatically, we select the 100 m-depth horizon as the outcrop surface in our yearly averaged model outputs and observational dataset. For each density layer we quantify the mean degree of oxygen saturation (percent) as the area weighted horizontally averaged oxygen saturation at the intercept of the isopycnal and the outcrop surface. Everywhere on the isopycnal we compute $O_{2\ sat}$, the oxygen concentration ($\text{mmol}\,\text{m}^{-3}$) equivalent to 100 percent saturation, given local potential temperature and salinity (Weiss, 1970). Local preformed oxygen concentration $O_{2\ pre}$ is inferred by multiplying local $O_{2\ sat}$ with the mean degree of oxygen saturation (as defined above), for that isopycnal. Consequently the mean degree of oxygen saturation (percent) is constant on a given isopycnal while the preformed oxygen concentration may vary along the isopycnal. This procedure is repeated for all density layers and EOU is ultimately determined for every grid box as $O_{2,pre}$ minus $O_{2\ obs}$.

A critical parameter is the number of isopycnal layers considered. Indeed, few (many) isopycnal layers imply strong (weak) diapycnal mixing in the interior ocean. We find that dividing the ocean in 10 isopycnal layers of equal density width ($1\,\text{kg}\,\text{m}^{-3}$) from 1020

Discussion Paper | Discussion Paper | Discussion Paper | Discussion Paper |

BGD

10, 2245–2267, 2013

The EOU: a new estimate of oxygen utilization

O. Duteil et al.

to 1030 kg m^{-3} leads to the best TOU estimate (Fig. A1). This is the number of layers which we apply in this study.

The conceptual script used to compute the Evaluated Oxygen Utilization is given below :

```
Variables
dens : potential density of a water parcel
mindens : minimum potential density of the water column
maxdens : maximum potential density of the water column
denslayer : thickness of the density layer
zlevel : vertical level
inidepth : depth at which computation starts
maxdepth : greatest depth of the water column
numpoints : number of points at a given depth belonging to the same dens. layer
minpoints : min. number of points required to assess a dens. layer to
a saturation percent.
oxygen : O2 concentration
100sat : O2 concentration if the water column is 100 percent saturated
evalpref: evaluated O2 concentration of a density layer (pref. O2 in the EOU approach)

Constant values
denslayer = 1
minpoints = 10
inidepth = 100

1.Discretize the ocean in density layers
FOR dens = mindens TO maxdens STEP denslayer

2. Mask the ocean outside the considered 'isodensity' volume
IF (dens - denslayer) / 2 LT dens LT (dens + denslayer) / 2 THEN mask = 1 ELSE mask = NaN

3.Compute the mean saturation of the shallower part of the isodensity volume
FOR zlevel = inidepth TO maxdepth
 numpoints = SUM(mask(zlevel))
 IF numpoints GT minpoints THEN surfsat = MEAN(mask * oxygen / 100sat) EXITFOR
ENDFOR EACH zlevel

4. Apply the mean saturation to the whole isodensity volume
FOR EACH zlevel
 evalpref = mask * surfsat * 100sat
ENDFOR EACH zlevel

ENDFOR dens
```


BGD
10, 2245–2267, 2013

Appendix B

Upper ocean oxygen disequilibrium in the observational dataset and model outputs

The most significant atmosphere/upper ocean oxygen disequilibrium occurs in the high latitude subduction regions, where deep water (considered here as the water denser than 1027.5 kg m^{-3}) forms. This deep water subducts both in the southern ocean (Circumpolar Deep Water: CDW) and in the northern North Atlantic (NADW: North Atlantic Deep Water) (Fig. B1a).

In the observations, the annual mean oxygen field at 100 m depth (corresponding to the depth used to compute the preformed O_2 in the EOU approach) of the CDW is significantly undersaturated (mean saturation rate of 86 percents), particularly in the Ross and Wedell Sea (Gordon and Huber, 1990; Keeling et al., 2010). This disequilibrium is caused by limited contact of the surface ocean with atmosphere (sea ice cover, subduction rate significantly faster than air/sea exchange) and transport of low oxygenated water from the deep ocean. The north Atlantic regional annual mean oxygen saturation at 100 m depth is higher and close to saturation (Fig. B1b).

In the models studied here, the degree of saturation at the outcrop of the NADW is high and above 90 percent. Concerning the southern ocean, models can be classified in two groups. In MOM P2A, MIT28 and ECCO2, the CDW is well oxygenated at 100 m depth (mean saturation degree higher than 90 percent), while in CSIRO, om1p7-BLINGv0 and UVIC the mean oxygen saturation degree is lower than estimated for the observations (values ranging from 75 to 85 percent). A possible cause of the differences between models is linked to the intensity of diapycnal mixing in the ocean interior, which controls the overturning strength, and consequently the subduction rate (Gnanadesikan, 1999).

BGD
10, 2245–2267, 2013

Acknowledgements. We acknowledge financial support to O. D., A. O. and I. K. from the Deutsche Forschungsgemeinschaft (SFB 754), to W. K. from the German Federal Ministry of Education and Research (FKZ 03F0608A, BIOACID), to E. G. from Compute Canada, to R. M. from the funding support of the Australian Climate Change Science Program. The research of D. B. was funded by Canadian Institute for Advanced Research (CIFAR) Earth System Evolution program. The research of E. G. was funded by the Natural Sciences and Engineering Research Council (NSERC) and the Canadian Institute for Advanced Research (CIFAR).

The service charges for this open access publication have been covered by a Research Centre of the Helmholtz Association.

References

Anderson, L. A. and Sarmiento, J. L.: Global ocean phosphate and oxygen simulations, Global Biogeochem. Cy., 9, 621–636, doi:10.1029/95GB01902, 1995. 2246, 2247

DeVries, T., Primeau, F., and Deutsch, C.: The sequestration efficiency of the biological pump, Geophys. Res. Lett., 39, L13601, doi:10.1029/2012GL051963, 2012. 2253

Dietze, H. and Oschlies, A.: Modeling abiotic production of apparent oxygen utilisation in the oligotrophic subtropical North Atlantic, Ocean Dynam., 55, 28–33, 2005. 2248

Duteil, O., Koeve, W., Oschlies, A., Aumont, O., Bianchi, D., Bopp, L., Galbraith, E., Matear, R., Moore, J. K., Sarmiento, J. L., and Segschneider, J.: Preformed and regenerated phosphate in ocean general circulation models: can right total concentrations be wrong?, Biogeosciences, 9, 1797–1807, doi:10.5194/bg-9-1797-2012, 2012. 2246, 2247, 2251

Feely, R., Sabine, C., Lee, K., Berelson, W., Kleypas, J., Fabry, V., and Millero, F.: Impact of anthropogenic CO_2 on the $CaCO_3$ system in the oceans, Science, 305, 362–371, 2004. 2246, 2247

Galbraith, E. D., Gnanadesikan, A., Dunne, J. P., and Hiscock, M. R.: Regional impacts of iron-light colimitation in a global biogeochemical model, Biogeosciences, 7, 1043–1064, doi:10.5194/bg-7-1043-2010, 2010. 2248

Garcia, H. E., Locarnini, R. A., Boyer, T. P., Antonov, J. I., Baranova, O. K., Zweng, M. M., and Johnson, D. R.: World Ocean Atlas 2009, vol. 3: Dissolved Oxygen, Apparent Oxygen Utilization, and Oxygen Saturation, edited by: Levitus, S., NOAA Atlas NESDIS 70, US Government Printing Office, Washington, D.C., 344 pp., 2010. 2249

Gebbie, G. and Huybers, P.: How is the ocean filled?, Geophys. Res. Lett., 38, L06604, doi:10.1029/2011GL046769, 2011. 2252

Gnanadesikan, A.: A simple model for the structure of the oceanic pycnocline, Science, 283, 2077–2079, 1999. 2256

Gnanadesikan, A., Dunne, J., Key, R., Matsumoto, K., Sarmiento, J., Slater, R., and Swathi, P.: Oceanic ventilation and biogeochemical cycling: understanding the physical mechanisms that produce realistic distributions of tracers and productivity, Global Biogeochem. Cy., 18, GB4010, doi:10.1029/2003GB002097, 2004. 2248

Gordon, A. and Huber, B.: Southern ocean mixed layer, J. Geophys. Res.-Oceans, 95, 11655–11672, 1990. 2246, 2256

Ito, T. and Follows, M.: Preformed phosphate, soft tissue pump and atmospheric CO_2, J. Mar. Res., 63, 813–839, 2005. 2247, 2253

Ito, T., Follows, M., and Boyle, E.: Is AOU a good measure of respiration in the oceans?, Geophys. Res. Lett., 31, L17305, doi:10.1029/2004GL020900, 2004. 2247, 2248, 2250

Keeling, R. F., Koertzinger, A., and Gruber, N.: Ocean deoxygenation in a warming world, Annu. Rev. Mar. Sci., 2, 19929, doi:10.1146/annurev.marine.010908.163855, 2010. 2246, 2247, 2256

Koeve W.: Wintertime nutrients in the North Atlantic – new approaches and implications for estimates of seasonal new production, Mar. Chem., 74, 245–260, doi:10.1016/S0304-4203(01)00016-0, 2001. 2246

Koertzinger, A., Schimanski, J., and Send, U.: High-quality oxygen measurements from profiling floats: a promising new technique, J. Atmos. Ocean. Technol., 22, 302–308, 2005. 2246

Khatiwala, K.: A computational framework for simulation of biogeochemical tracers in the ocean, Global Biogeochem. Cy., 21, GB3001, doi:10.1029/2007GB002923, 2007. 2248

Kriest, I., Khatiwala, K., and Oschlies, A.: Assessment of simple global marine biogeochemical models of increasing complexity, Prog. Oceanogr., 86, 336–360, 2010. 2248, 2251

Marinov, I., Gnanadesikan, A., Sarmiento, J., Toggweiler, J., Follows, M., and Mignone, B.: Impact of oceanic circulation on biological carbon storage in the ocean and atmospheric pCO_2, Global Biogeochem. Cy., 22, GB3007, doi:10.1029/2007GB00295810.1029/2007GB002958, 2008. 2253

Matear, R. and Hirst, A.: Long-term changes in dissolved oxygen concentrations in the ocean caused by protracted global warming, Global Biogeochem. Cy., 17, GB4008, doi:10.1029/2002GB001997, 2003. 2248

Oschlies, A., Schulz K., Riebesell U., and Schmittner, A.: Simulated 21st century's increase in oceanic suboxia by CO_2-enhanced biotic carbon export, Global Biogeochem. Cy., 22, GB1125, doi:10.1029/2007GB003147, 2008. 2248

Pahlow, M. and Riebesell, U.: Temporal trends in deep ocean Redfield ratios, Science, 287, 831–832, 2000. 2246, 2247

Redfield, A. C., Ketchum, B. H., and Richards, F. A.: The influence of organisms on the composition of seawater, in: The Sea, vol. 2, edited by: Hill, M. N., John Wiley and Sons, New York, 26–77, 1963. 2246, 2247

Russell, J. L. and Dickson, A. G.: Variability in oxygen and nutrients in South Pacific Antarctic Intermediate Water, Global Biogeochem. Cy., 17, 1033, doi:10.1029/2000GB001317, 2003. 2246

Sarmiento, J. L. and Gruber, N.: Ocean Biogeochemical Dynamics, Princeton University Press, Princeton, NJ, 526 pp., 2006. 2246, 2247

Stammer, D., Ueyoshi, K., Kohl, A., Large, W. G., Josey, S. A., and Wunsch, C.: Estimating air-sea fluxes of heat, freshwater, and momentum through global ocean data assimilation, J. Geophys. Res., 109, C05023, doi:10.1029/2003JC002082, 2004. 2249

Stommel, H.: Determination of water mass properties of water pumped down from the Ekman layer to the geostrophic flow below, P. Natl. Acad. Sci. USA, 76, 3051–3055, 1979. 2252

Weiss, R.: The solubility of nitrogen, oxygen, and argon in water and seawater, Deep-Sea Res., 17, 721–756, 1970. 2254

Table 1. Main characteristics of the models analyzed in this study.

Model	MOM-P2A	CSIRO	om1p7-BLINGv0	UVIC	TMM-MIT28	TMM-ECCO2
Resolution	3.75 × 4	3.2 × 5.6	0.6 (eq) to 2 × 3	3.6 × 3.6	2.8 × 2.8	1 × 1
Vertical levels	24	21	28	19	15	23
Integration type	online	online	online	online	offline	offline
Wind stress	ECMWF	Previous coupled exp.	CORE	NCEP-NCAR	NCEP-NCAR	CORE
Biology Boxes	OCMIP(N) 4 PO_4, (implicit PZD), O_2, DIC, TALK	N 4 PO_4, (implicit PZD), O_2, DIC, TALK	N 4 PO_4, (implicit PZD), O_2, DOP, iron	NPZD 9 2 phy., 1 zoo., NO_3, PO_4, Detritus, O_2, DIC, TALK	NPZD 6 1 phy., 1 zoo., PO_4, DOP, DOM, O_2	NPZD 6 1 phy., 1 zoo., PO_4, DOP, DOM, O_2
Ref.	Gnanadesikan et al. (2004)	Matear and Hirst (2003)	Galbraith et al. (2010)	Oschlies et al. (2008)	Kriest et al. (2010)	Kriest et al. (2010)

BGD
10, 2245–2267, 2013

The EOU: a new estimate of oxygen utilization

O. Duteil et al.

Table 2. Oxygen utilization (mmol m^{-3}) and regenerated over total phosphate ratio (r/tot) computed from AOU, TOU and EOU for different model outputs and WOA dataset.

Model or dataset	MOM-P2A	CSIRO	om1p7-BLINGv0	UVIC	TMM-MIT28	TMM-ECCO2	WOA
AOU	142.8	147.7	186.2	156.4	141.9	164.6	153.0
TOU	121.4	129.6	120.7	119.8	130.4	140.1	
EOU	129.5	127.0	135.3	125.2	127.9	146.0	115.5
r/tot AOU	0.38	0.39	0.50	0.42	0.38	0.45	0.40
r/tot TOU	0.32	0.34	0.32	0.32	0.34	0.37	
r/tot EOU	0.34	0.34	0.36	0.33	0.34	0.39	0.30

BGD
10, 2245–2267, 2013

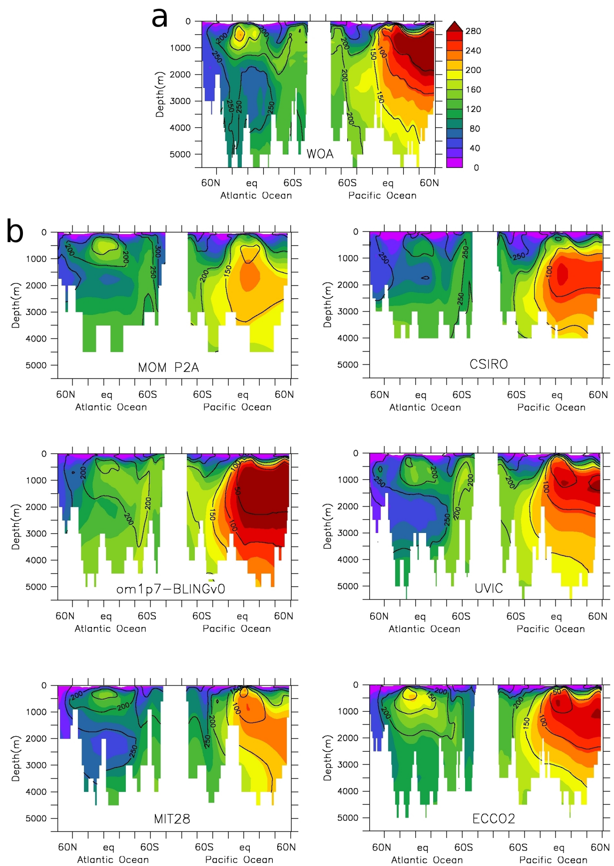

Fig. 1. Apparent Oxygen Utilisation (AOU) (mmol m^{-3}) along an Atlantic meridional section (30W) and Pacific meridional section (150W) in the WOA dataset **(a)** and in the model outputs **(b)**: MOM-P2A, CSIRO, om1p7-BLINGv0, UVIC, TMM-MIT28, TMM-ECCO2. Oxygen concentration (mmol m^{-3}) is traced in contour.

BGD
10, 2245–2267, 2013

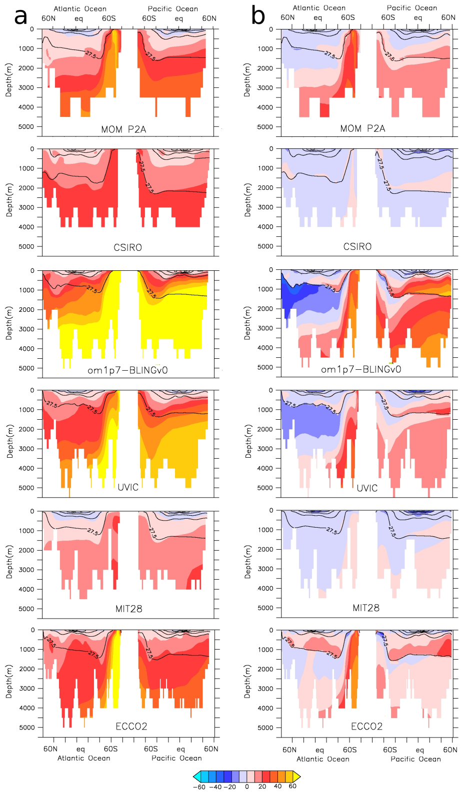

Fig. 2. (**a** – left panel) Apparent Oxygen Utilisation (AOU) – True Oxygen Utilisation (TOU) (mmol m^{-3}) and (**b** – right panel) Evaluated Oxygen Utilisation (EOU) – True Oxygen Utilization (TOU) (mmol m^{-3}) along an Atlantic meridional section (30° W) and Pacific meridional section (150° W) in different models: CSIRO, MOM-P2A, om1p7-BLINGv0, UVIC, TMM-MIT28, TMM-ECCO2. Levels of constant density are traced in contour.

BGD

10, 2245–2267, 2013

The EOU: a new estimate of oxygen utilization

O. Duteil et al.

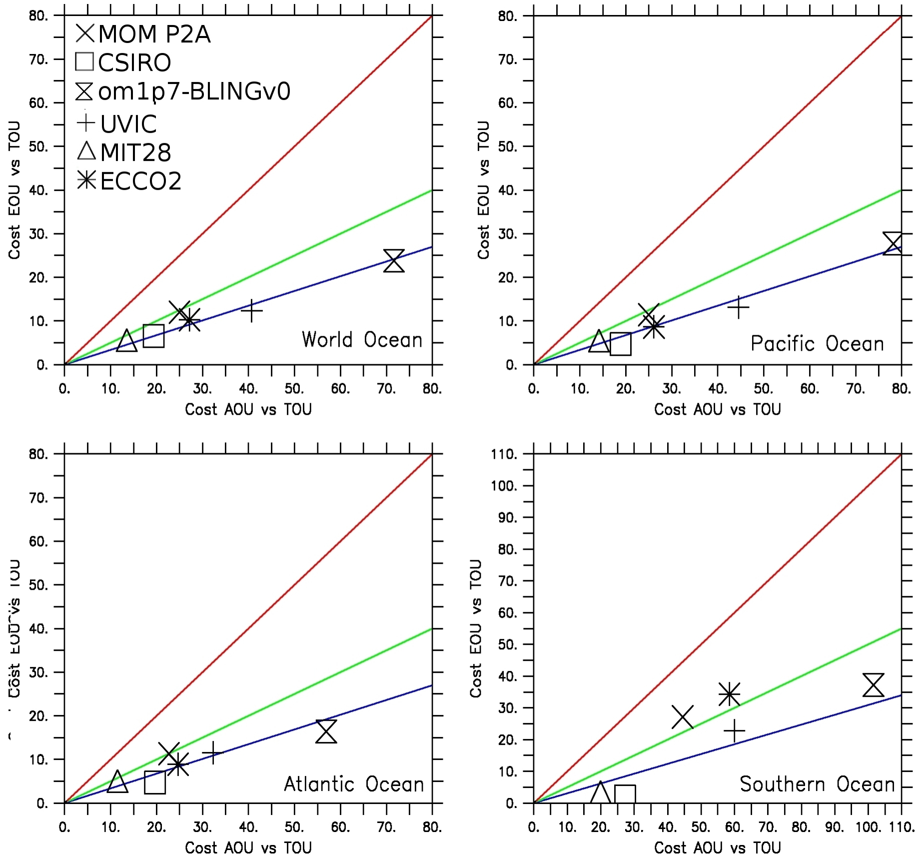

Fig. 3. RMS errors for AOU vs TOU (abscissae) and EOU vs TOU (ordinates) for the global ocean, Pacific, Atlantic and Southern Ocean. The red line is the 1 : 1 line, indicating that the performance of EOU and AOU to estimate TOU is equivalent. The green and blue lines represent the 2 : 1 and 3 : 1 lines, respectively. (EOU estimates TOU "twice better" and "three time better" than AOU). EOU has been computed using 10 isopycnal layers.

BGD
10, 2245–2267, 2013

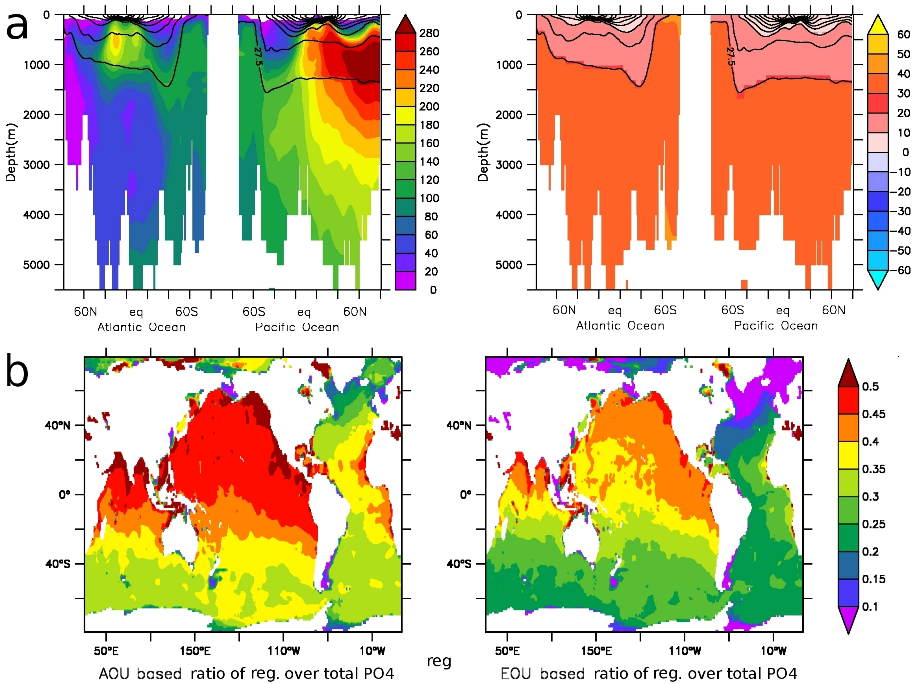

Fig. 4. (a) Evaluated Oxygen Utilization (EOU) (left) and AOU–EOU (right) ($mmol\,m^{-3}$) along an Atlantic meridional section (30° W) and Pacific meridional section (150° W) in WOA. **(b)** Averaged water column ratio of regenerated over total phosphate concentration computed using AOU (left) and EOU (right).

BGD
10, 2245–2267, 2013

The EOU: a new estimate of oxygen utilization

O. Duteil et al.

Title Page
Abstract
Introduction
Conclusions
References
Tables
Figures
◀
▶
Back
Close
Full Screen / Esc
Printer-friendly Version
Interactive Discussion

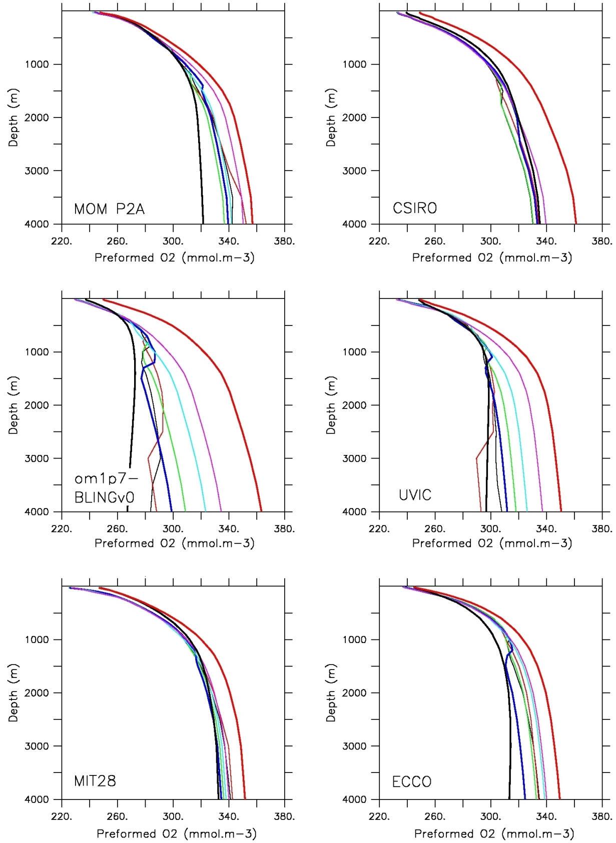

Fig. A1. Global mean profiles of preformed O_2 corresponding to TOU (bold black), AOU (bold red) and EOU in the different models: CSIRO, MOM-P2A, om1p7-BLINGv0, UVIC, TMM-MIT28, TMM-ECCO2. EOU has been computed considering a increasing number of density layers ranging from 3 to 25 (thin black: 25 layers, thin red: 20, green: 15, blue: 10, light blue: 5, magenta: 3).

BGD
10, 2245–2267, 2013

Title Page
Abstract | Introduction
Conclusions | References
Tables | Figures
◂| |▸
◂ ▸
Back | Close
Full Screen / Esc
Printer-friendly Version
Interactive Discussion

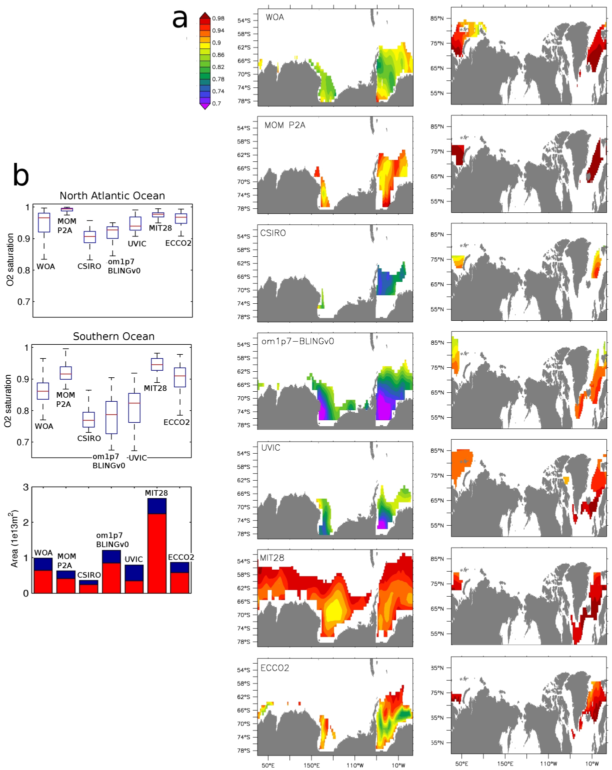

Fig. B1. (a) Box plot of volume weighted oxygen saturation in the Northern (top panel) and Southern (middle panel) Hemispheres, respectively, at 100 m depth and where the density is greater than 1027.5 kg m^{-3}. Lower panel shows the area in the Northern (blue) and Southern (red) Hemisphere where the density is greater than 1027.5 kg m^{-3}. **(b)** Distribution of oxygen saturation at 100 m depth in the southern (left) and northern (right) outcrop regions of water masses denser than 1027.5 kg m^{-3}.

BGD
10, 2245–2267, 2013

Title Page
Abstract | Introduction
Conclusions | References
Tables | Figures
◀| |▶
◀ ▶
Back | Close
Full Screen / Esc
Printer-friendly Version
Interactive Discussion